Landfill liner interface parameters and member selection with stability assessment, and factor of safety predictions with seismic loading

M. Saravanan[1], M. Kamon[2], H.A. Faisal[2], T. Katsumi[4], T. Akai[5], T. Inui[6], and A. Matsumoto[5]

[1)] Principal Engineer of Nexus Engineering Consultant, Malaysia.

[2)] Professor, Graduate School of Global Environmental Studies, Kyoto University, Japan

[3)] Professor, Department of Civil Engineering, University Malaya, Malaysia

[4)] Assoc Prof., Graduate School of Global Environmental Studies, Kyoto University, Japan

[5)] Senior Research Scientist, Technology Research Institute of Osaka Prefecture, Japan

[6)] Assist Prof., Graduate School of Global Environmental Studies, Kyoto University, Japan

*Corresponding author : vanan.nexus@gmail.com

ABSTRACT *: Research has be carried on the internal and interface shear strength properties of landfill liner components, which consist of subsoils, compacted clay liners (CCLs) , geosynthetic clay liners (GCLs), geomembrances and geotextiles. The soil-geomembrane or any other liner interface combination could act as a possible plane of potential instability of the liner under static and seismic loading (Hoe et al. 1997). Hence, this paper addresses part of our research to investigate the important factors, which should be considered by geotechnical engineers designing landfills, to prevent failures due to poor interface properties under static and earthquake induce forces (seismic loading) for both based and cover soil liners. Interface stress and horizontal strain behaviour for various liner configuration was studied to understand the peak and residual shear stress trend to select suitable liner configuration which can act as a composite member during failure. Understanding the stress and horizontal strain behaviour of liner member component is critical in order to allow the transfer of failure stress between interfacing member to resist continuous or progressive failure from occurring. The findings of the study are compiled into a simplified computation model to assist engineers in predicting and estimating the factor of safety (FOS) of the liner interface stability during design stages or for on-going filling work where the landfill geometry is continuously changing.*

Keywords : landfill liner, interface properties, factor of safety, geomembrance, geotextile, geosynthetic clay liners (GCLs), liner composite.

1. Introduction

Selecting the appropriate landfill liner depends mainly on the environmental protection regulations of an individual country, which often focus on protecting against leachate leakage. However, from geotechnical aspect, the landfill liner selection depends on the slope sections, fill heights, interface properties, and horizontal strain compatibilities. Tables 1a, 1b and 2 present various combinations of laboratory interface test results and interface stress and horizontal strain behaviour of the tests obtained from Saravanan et al., 2006c, respectively.

Stark et al. 1994, have presented design approach that uses a combination of the peak and residual shear strengths. However, the use of peak and residual shear strengths has uncertainty in the failure relationship between laboratory shear displacement, field shear displacement, the effect of progressive failure, and possible shear displacement due to an earthquake along the interface failure plane. Hence, various failure conditions required to be considered in interface design (Shark et al. 2004).

If more than one interface parameter is used to develop the failure envelope of a liner with the lowest peak and residual strength, then the failure envelope is referred to as a composite failure envelope. In summary, designers should reconsider the use of minimum peak and residual failure envelope for design by determining which material will reach the peak and residual shear stress condition earlier with horizontal strain and use the corresponding parameters for peak and residual composite failure envelope for design. This can be achieved by establishing the stress and horizontal strain behaviour of every individual interface component with normal stresses and then evaluate the composite failure envelope trend.

2.0 Liner interface stress and horizontal strain behaviour

Lower interface shear strengths between geomembranes and other geosynthetics can trigger a rapid failure during seismic loading conditions. Many researchers have discussed the interface shear strengths of landfill materials (e.g., Stark et al. 1994, Gilbert et al. 1996, Stark et al. 1996, Daniel et al. 1998, Palmeira et al. 2002, Chiu et al. 2004, Fox et al. 2004, Gourc et al. 2004, Kotake et al. 2004). The soil geomembrane interface acts as a potential plane of instability under both static and seismic loadings (Ling et al. 1997). Such interfaces have failed in the past due to low friction angle between the soil and the geosynthetic layers within the liner system. Therefore, the interface shear strength of any combination of liner materials requires meticulous study for safe design of new landfills. Hence, this paper examines some common landfill liner configurations in order to understand the possible modes of single and composite interface failure trend. Figure 1 shows the typical section of a landfill used to model the stability analysis. Figure 2a and 2b shows a typical landfill liner configuration for base and cover liner. Peak shear stress with strain plot for the configuration in Figure 2a is shown in Figure 4a and 4b.

Figures 3a, 3b, 3c, 3d and 3e shows typical analysis results for the cases listed in Table 3. Seismic horizontal coefficients of 0.5, 0.1, 0.15, 0.2 and 0.25 were introduced in the analysis in order to study the trend of liner interface performance under earthquake-induced loading.

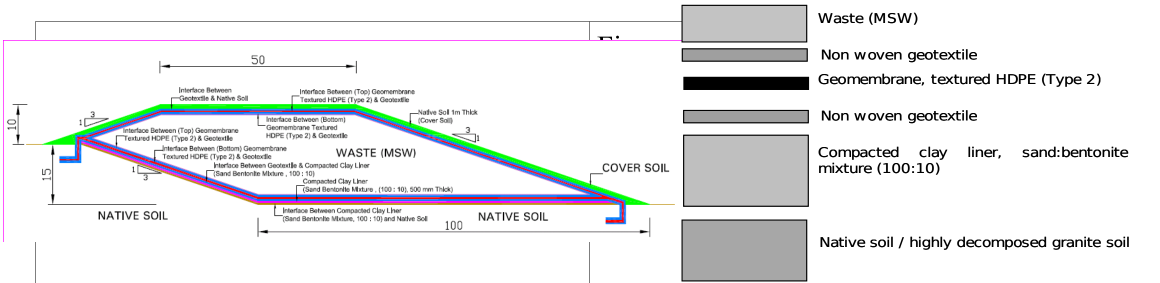

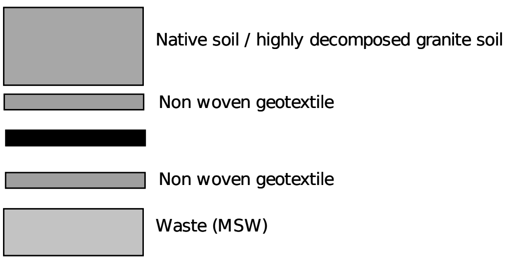

Figure 2b : Configuration of single membrane cover liner.

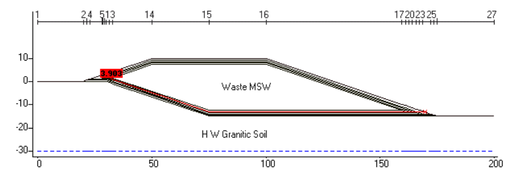

Figure 3(a) : Typical failure section within the bottom liner in Cases 1 to 5.

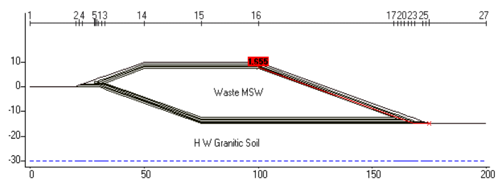

Figure 3(b) : Typical failure section within the landfill covers in Cases 6 to 9

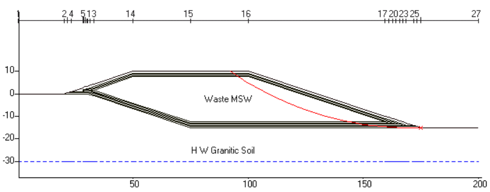

Figure 3 (c) : Toe failure of waste - Case 10

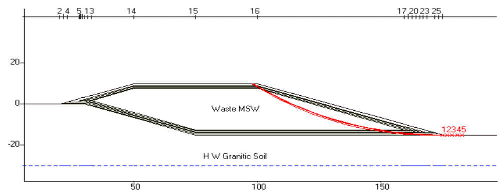

Figure 3 (d) : Overall landfill failure - Case 11

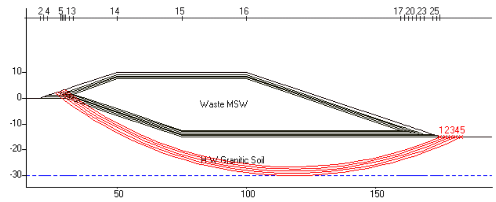

Figure 3 (e) : Overall landfill base failure - Case 12

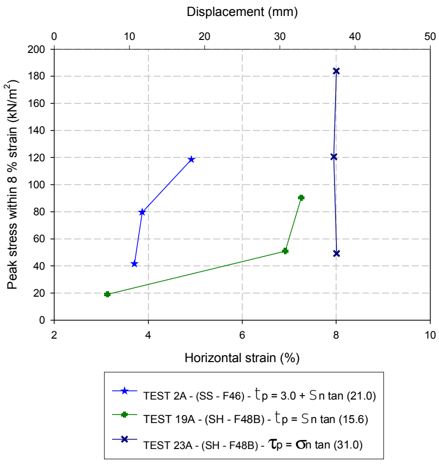

Figure 4a : Peak shear stress with strain plot for the configuration in Figure 2a.

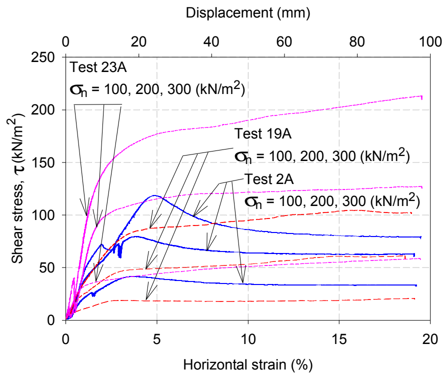

Figure 4b : Stress strain behaviour for the bottom liner shown in Figure 2a.

3.0 Landfill liner and cover interface stability prediction

To simplify the interface stability evaluation, data were complied to produce a computational model and graph to assist engineers to predict the interface FOS of a landfill liner and landfill cover during the design stages and also during the service stages.

The FOS is computed by dividing resisting forces against passive forces such as the shear strength of a failure plane and other stabilizing forces acting on the wedge. By using the Mohr Coulomb criteria

$$\tau = c + \sigma_n \tan\varphi \qquad (1)$$

$$F = \frac{cL + W\cos\alpha\tan\varphi}{W\sin\alpha} \qquad (2)$$

The above equation is further simplified by computing fictional and cohesion contributions individually.

Friction Contribution:

$$FOS_F = \frac{\tan\varphi}{\tan\alpha} \qquad (3)$$

Cohesion Contribution:

$$FOS_C = \frac{cL}{W\sin\alpha} \qquad (4)$$

As for the frictional contribution from equation 3, progressive failure could occur in slopes of which the driving force exceeds the mobilized strength of the weakest layer, for example when the slope angle exceeds the friction angle of the interface (Mesri et al., 2003). In contrast to the frictional resistance, the cohesional contribution completely depends on the cover height and contact area per unit length. Hence, it is important to balance both cohesional and frictional contribution for FOS under the limit equilibrium design.

3.1 Seismic influence on landfill base and cover liner factor of safety

Seismic effects are incorporated in the limit equilibrium analysis where the forces induced by earthquake accelerations were treated as horizontal forces. Although vertical forces are also caused by an earthquake, these forces were not computed into the analysis. The horizontal force (F_h), due to an earthquake is assumed to act through the centre of gravity of soil mass involved in predicting the failure as:

$F_h = kw = k\ mg$ (5)

Where m is the mass of the soil and k is the seismic coefficient. Thus, the seismic coefficient k is a measurement of the earthquake acceleration in terms of g. Table 4 shows the calculation, while Figure 5 shows the computation model for base liner stability.

FOS from Friction= $FOS_F = \tan\varphi * (P/A)$ (6)

FOS from Cohesion = $FOS_C = \tan\varphi * (L/A)$ (7)

Total FOS = $FOS_F + FOS_C$ (8)

Where P is the Passive Resistance, A is the Active Forces, and L is the Total Interface Length. In order to understand, predict, and monitor the continuous trend of the FOS during filling and maintenance work, each FOS is computed individually based on the frictional and cohesional contributions. Figures 6a and 6b show the individual plots of the FOS based on the frictional and cohesional contributions, respectively, with the coefficient of active forces and passive resistance incorporated.

The frictional contribution of the FOS tends to have an exponential increment with friction angle. As shown in Figure 6a, the higher the value of passive resistance against active forces (P/A) the higher the FOS. However in Figure 6b the FOS increases linearly with cohesion. The incorporated plot of the Interface Length/Active Forces (L/A) allows the FOS to be estimated based on cohesion parameters. The total predicted FOS can be low as 1.1 or 1.3 as the computed coefficients of P/A and L/A has incorporated all the active and destabilising forces, including seismic loading.

Similar prediction plot was also made for a cover slope for P/A and L/A in Figure 8a and 8b respectively. Table 5 shows the sample calculation for the cover liner interface computation model shown in Figure 7. The toe passive resistance was ignored in the computation. In the case of the cover slope, the friction contribution has a minor contribution to the total FOS.

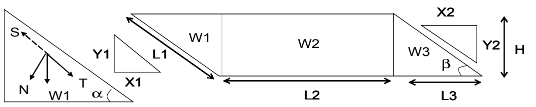

Figure 5 : Landfill base liner interface stability computation model.

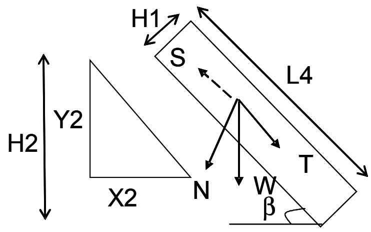

Figure 7 : Landfill cover liner interface stability computation model.

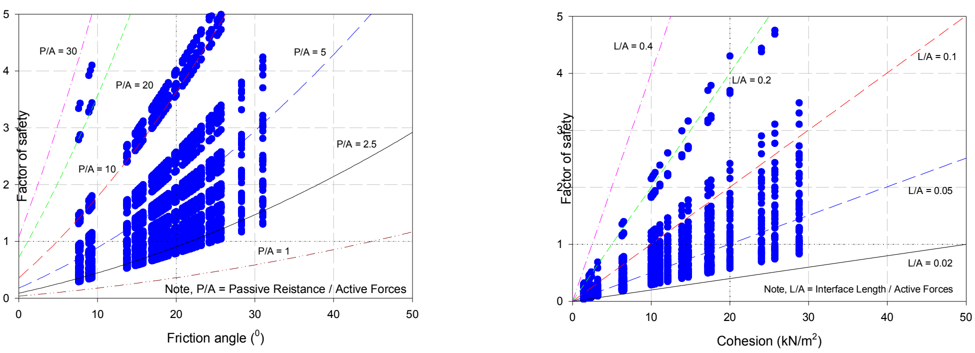

Figure 6a : Prediction of interface FOS based on P/A (Passive Resistance/Active Forces) for base liner stability for frictional resistances.

Figure 6b : Prediction of interface FOS based on L/A (Interface Length/Active Forces) for base liner stability for cohesional resistance.

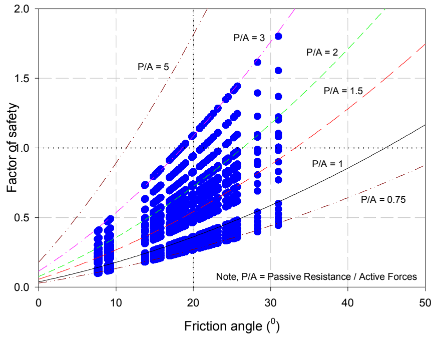

Figure 8a : Prediction of interface FOS based on P/A (Passive Resistance/Active Forces) for cover slope stability for frictional resistance.

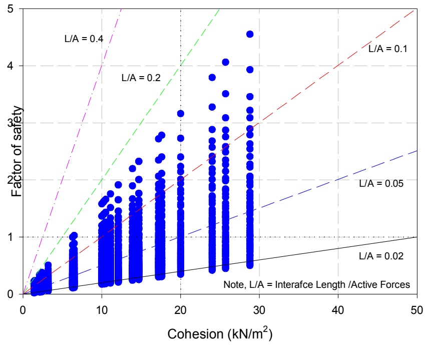

Figure 8b : Prediction of interface FOS based on L/A (Interface Length/Active Forces) for cover slope stability for cohesional resistance.

4 Conclusion

As for liner design, it is recommended to configure the liner members to act as a composite member during failure. The composite behaviour could cause the failing interface plane to cut through other interface planes and indirectly gain resisting strength during failure. Hence, understanding the stress and horizontal strain behaviour of liner member components is critical in order to allow the transfer of failure stress between interfacing members to resist continuous or progressive failure from occurring. The proposed method to analyze the interface stress and horizontal strain behaviour in order to understand the failure trend could assist design engineers in evaluating the performance of an individual interfacing member, which may identify the possibility of a composite or non-composite failure mode based on fill height (normal stresses). This evaluation would improve the selection of liner members, the orientation or placement methodology, and the material properties.

As for frictional and cohesional contributions of the interface parameters, it is recommended to introduce an interfacing liner with a higher cohesional contribution compared to frictional resistance for cover soil liners due to the low normal loads (shallow fill height). However, for bottom liners, frictional resistance had significant influence on interface stability due to high normal loads and counter balancing geometry. Along with stability and interface property assessment engineers are required to carefully select the liner configuration with a suitable stress and horizontal strain behaviour at the preliminary peak stages and at the post peak stresses in the residual region in order to design a well-integrated composite design.

The FOS assessment depends on the landfill geometry, liner interface properties, and external disturbing forces such as seismic loading. Hence, engineers are required to balance the active and passive resistance forces (P/A), and the interface length with active forces (L/A) to prevent a sudden and drastic drop in the FOS during an earthquake. Hence, it is vital to continuously assess the FOS or to monitor the FOS while filling to ensure the landfill sites are stable at all times in order to resist external destabilizing forces. This finding also indicates that not all safe slopes are actually stable under seismic conditions, when it comes to an interface induced failure. Hence, the proposed FOS prediction method could be a useful guide for engineers. The advantage of the proposed FOS prediction methods are:

- Will be quick reference for engineers when selecting liner materials based on interface test properties.
- Can obtain initial estimation of the FOS based on site geometry or back slope conditions.
- Useful for designing the appropriate anchorage methods for liners to obtain an adequate FOS.
- Useful to perform continuous monitoring of the FOS at a landfill site while filling work are in progress.
- Assist in organizing a sequential filling to maintain an adequate FOS for both static and

seismic conditions.

- If the FOS is found to be inadequate appropriate steps can be taken immediately to avoid sudden failures by reorganising the filling lift to provide sufficient counter balance.
- Useful for site engineers to safely coordinate ongoing filling work.

5 REFERENCES

Chiu, P. and Fox, P.J. (2004). Internal and interface shear strengths of unreinforced and needle-punched geosynthetic clay liners, *Geosynthetics International,* 11, No.3, 176–199.

Daniel, D.E. Koerner, R.M., Bonaparte, R., Landreth, R.E., Carson, D.A., and Scranton, H.B. (1998). Slope stability of geosynthetic clay liner test plots, *Journal of Geotechnical and Geoenvironmental Engineering,* ASCE, 124, No.7, 628-637.

Fox, P. J. and Stark, T. D. (2004). State-of-the-art report: GCL shear strength and its measurement, *Geosynthetics International,* 11, No.3, 141–175.

Gilbert, R. B. and Byrne, R. J. (1996). Strain-softening behavior of waste containment system interfaces. *Geosynthetics International*, 3. No. 2, 181-203.

Gourc, J.P. and Reyes Ramirez, R. (2004). Dynamics-based interpretation of the interface friction test at the inclined plane, *Geosynthetics International,* 11, No.6, 439–454.

Hoe I. Ling and Dov Leshchinsky, (1997). Seismic stability and permanent displacement of landfill cover systems, *Journal of Geotechnical and Geoenvironmental Engineering*, pp. 113-112.

Kotake, N., Watanabe, K., Nonomura, C., and Negishi, K. (2004): Interactive behaviors of geosynthetics multi-layer systems under shear force, *GeoAsia2004, Proceedings of the 3rd Asian Regional Conference on Geosynthetics,* J.B. Shim, C. Yoo, and H.-Y. Jeon (eds.), 937-944.

Ling, H.I. and Leshchinsky, D. (1997). Seismic stability and permanent displacement of landfill cover systems, *Journal of Geotechnical and Geoenvironmental Engineering,* ASCE, 123, No.2, 113-122.

Mesri, G. and Shahien, M. (2003). Residual shear strength mobilized in first-time slope failures: *Journal of Geotechnical and Geoenvironmental Engineering*, ASCE, 129, No. 1, 12-31.

Palmeira, E.M., Lima, N. R. Jr, and Mello, L.G.R. (2002). Interaction between soils and geosynthetic layers in large-scale ramp tests, *Geosynthetics International,* .9, No.2, 149–187

Reddy, K. R., Kosgi, S. & Motan, S. (1996). Interface shear behavior of landfill composite liner systems: a finite element analysis. *Geosynthetics International,* 3, No. 2, 247-275.

Saravanan M., Kamon M., Faisal H. A., Katsumi T., Akai T., Inui T., Matsumoto A. (2006c). Interface performances of geotextiles, geomembranes, GCLs and CCLs for landfill liner stability. *Geotextitle and Geomembrane* (under review)

Stark, T. D. and Choi H. (2004). Peak versus residual interface strengths for landfill liner and cover design. *Geosynthetics International*, 11, No. 6, 491-498

Stark, T. D. and Poeppel, A. R. (1994). Landfill liner interface strengths from torsional ring shear tests. *Journal of Geotechnical Engineering*, ASCE, 120, No. 3, 597-615.

Stark, T. D., Williamson, T. A. and Eid, H. T. (1996). HDPE geomembrane/geotextile interface shear strength. *Journal of Geotechnical Engineering*, ASCE, 122, No.3, 197-203.

6 NOTATION

L	=	Length of failure plane
τ	=	Total shear strength
c	=	Total cohesion
W	=	Total weight acting on the failure plane
α	=	Side slope angle
β	=	Cover slope angle
ϕ	=	Total friction angle
N	=	Normal load
F_h	=	Horizontal force
m	=	Mass of waste
k	=	Seismic coefficient
g	=	Gravity acceleration
H	=	Fill height
H1	=	Cover fill height
H2	=	Cover slope height

σ_n = Total normal stress on failure plane
F = Factor of safety
P1, P2, P3 = Passive forces on individual landfill blocks
P = Total passive force
A1, A2, A3 = Active forces on individual landfill blocks
A = Total active force

W1, W2, W3 = Landfill block total weight
X1, X2 = Horizontal distance
Y1, Y2 = Vertical distance
L1, L2, L3 = Length of interface failure plane in a landfill block
L4 = Cover liner interface length
S = (W1) * cos (α or β)
T = (W1) * sin (α or β)

Table 1a : Various combinations of the laboratory interface tests.

Interfacing material	Geotextile	Smooth HDPE (Type 1)	Textured HDPE (Type 2)	Rear side of PVC	Front side of PVC	Bentonite side of bentonite -glued GCL (Type 1)	HDPE side of bentonite -glued GCL (Type 1)	Non woven side of needle-punched GCL (Type 2)	Woven side of needle-punched GCL (Type 2)	Native soil
Smooth HDPE (Type 1)	Test 1A									
Textured HDPE (Type 2)	Test 2A									
Rear side of PVC	Test 3A									
Front side of PVC	Test 3C									
Bentonite side of bentonite-glued GCL (Type 1)	Test 4A	Test 6A	Test 8A	Test 10A	Test 10E					
HDPE side of bentonite-glued GCL (Type 1)	Test 4C	Test 6C	Test 8C	Test 10C	Test 10G					
Non woven side of needle-punched GCL (Type 2)	Test 5A	Test 7A	Test 9A	Test 11A	Test 11E					
Woven side of needle-punched GCL (Type 2)	Test 5C	Test 7C	Test 9C	Test 11C	Test 11G					
Silt:bentonite mixture (100 : 10)	Test 12A	Test 13A	Test 14A	Test 15A	Test 15C	Test 17A	Test 17C	Test 18A	Test 18C	Test 16A
Sand:bentonite mixture (100 : 10)	Test 19A	Test 20A	Test 21A	Test 22A	Test 22C	Test 24A	Test 24C	Test 25A	Test 25C	Test 23A
Native soil	Test 26A	Test 27A	Test 28A	Test 29A	Test 29C					

Table 1b : Various combinations of the laboratory interface test results.

Interfacing material c: cohesion in kN/m^2 ϕ: frictional angle in degree.	Geotextile		Smooth HDPE (Type 1)		Textured HDPE (Type 2)		Rear side of PVC		Front side of PVC		Bentonite side of bentonite -glued GCL (Type 1)		HDPE side of bentonite -glued GCL (Type 1)		Non woven side of needle-punched GCL (Type 2)		Woven side of needle-punched GCL (Type 2)		Native soil	
	c	ϕ	c	ϕ	c	ϕ	c	ϕ	c	ϕ	c	ϕ	c	ϕ	c	ϕ	c	ϕ	c	ϕ
Smooth HDPE (Type 1)	0.0	7.6																		
Textured HDPE (Type 2)	3.0	21.0																		
Rear side of PVC	11.3	18.6																		
Front side of PVC	26.3	16.9																		
Bentonite side of bentonite-glued GCL (Type 1)	11.5	17.2	0.0	9.0	28.9	18.7	19.0	17.7	0.0	24.5										
HDPE side of bentonite-glued GCL (Type 1)	0.0	21.8	2.2	8.9	0.0	19.8	11.8	20.0	0.0	25.1										
Non woven side of needle-punched GCL (Type 2)	1.3	15.0	2.3	7.7	10.4	25.4	17.0	15.2	11.0	17.0										
Woven side of needle-punched GCL (Type 2)	10.6	14.7	2.4	9.2	2.5	22.9	14.4	18.0	22.8	18.4										
Silt:bentonite mixture (100 : 10)	0.0	15.2	0.0	15.3	0.0	24.1	0.0	22.2	0.0	19.8	13.9	16.9	0.0	22.5	6.1	20.8	1.7	21.2	10.3	28.3
Sand:bentonite mixture (100 : 10)	0.0	15.6	0.0	13.7	0.0	24.5	0.0	19.7	0.0	16.9	6.7	17.4	15.3	13.5	0.0	22.6	0.0	22.4	0.0	31.0
Native soil	0.0	17.8	0.0	15.6	0.0	23.0	0.0	18.7	0.0	20.2										

Table 2 : Interface stress strain behaviour of the interface test results.

Interfacing material	Geotextile	Smooth HDPE (Type 1)	Textured HDPE (Type 2)	Rear side of PVC	Front side of PVC	Bentonite side of bentonite -glued GCL (Type 1)	HDPE side of bentonite -glued GCL (Type 1)	Non woven side of needle-punched GCL (Type 2)	Woven side of needle-punched GCL (Type 2)	Native soil
Smooth HDPE (Type 1)	SH – F13 0.7-0.9*									
Textured HDPE (Type 2)	SS – F35 3.7-4.9*									
Rear side of PVC	SH – F48B 5.1-8.0B*									
Front side of PVC	SC – F48B 5.6-8.0B*									
Bentonite side of bentonite-glued GCL (Type 1)	SS – F35 4.1-4.8*	SH - F13 1.1-1.8*	SC - F35 3.0-3.8*	SH – F48B 5.6-8.0B*	SH - F13 1.6-8.0B*					
HDPE side of bentonite-glued GCL (Type 1)	SS – F35 4.2-4.5*	SH – F48B 7.8-8.0B*	SH – F35 3.4-4.1*	SH - F13 1.0-1.4*	SH - F13 1.7-2.0*					
Non woven side of needle-punched GCL (Type 2)	SS – F35 3.1-4.0*	SH - F13 1.1-1.6*	SS – F35 3.1-4.5*	SH - F46 4.6-6.1*	SH – F48 4.4-7.8*					
Woven side of needle-punched GCL (Type 2)	SH – F35 3.9-4.4*	SH - F13 0.9-1.6*	SS – F35 2.7-4.1*	SC - F48 5.1-8.0*	SC – F48B 4.2-8.0B*					
Silt:bentonite mixture (100:10)	SH – F46 4.5-5.7*	SH - F13 1.2-1.9*	SC – F48B 5.0-8.0B*	SC – F48 3.3-7.9*	SC – F48 3.4-7.8*	SH - F46 4.4-6.0*	SC – F48B 5.7-8.0B*	SC – F48 5.8-7.2*	SC – F48 5.5-7.8*	SH – F48B 7.8-8.0B*
Sand:bentonite mixture (100:10)	SH – F48 3.1-7.3*	SH - F13 0.8-1.9*	SH – F48B 8.0B*	SC – F48B 5.8-8.0B*	SC – F48B 3.8-8.0B*	SH – F13 2.5-3.6*	SC – F48B 5.6-8.0B*	SC – F48B 4.0-8.0B*	SC – F48B 6.7-8.0B*	SH – F48B 8.0B*
Native soil	SC – F48 4.2-7.9*	SH - F13 1.1-2.8*	SH – F48B 7.0-8.0B*	SC - F35 2.8-4.7*	SC - F35 1.7-3.0*					

SH: Horizontal strain hardening behavior for all normal stress levels tested.
SS: Horizontal strain softening behavior for all normal stress levels tested.
SC: Stress and horizontal strain behavior depends upon the normal stress levels. Horizontal strain hardening for low normal stress and softening for high normal stress.
F13, F35, or F46: Failure occurred within the 1-3%, 3-5%, or 4-6% of horizontal strain respectively.
F48B: Failure occurred within the 4-8% horizontal strain or beyond.
* - Horizontal strain at peak shear stress

Table 3: Stability cases considered for analysis.

Case	Description
Case 1	Interface falure between compacted clay liner – Sand:bentonite mixture (100:10) and native soil
Case 2	Internal failure of compacted clay liner – Sand:bentonite mixture (100:10)
Case 3	Interface failure between compacted clay liner – Sand:bentonite mixture (100:10) and geotextile
Case 4	Interface between geotextile and geomembrane Textured HDPE (Type 2) – Bottom
Case 5	Interface between geotextile and geomembrane Textured HDPE (Type 2) – Top
Case 6	Interface between geotextile and cover soil (highly weathered granitic soil – native soil)– Top
Case 7	Interface between geotextile and geomembrane Textured HDPE (Type 2) – Top
Case 8	Interface between geotextile and geomembrane Textured HDPE (Type 2) – Bottom
Case 9	Internal failure of cover soil (highly weathered granitic soil – native soil)
Case 10	Toe failure of waste
Case 11	Overall landfill failure
Case 12	Overall landfill base failure

Table 4: Computations approach for the landfill liner interface stability.

Passive Resistance	Active Forces
(W1)*cos α = P1 kN/m	(W1)*sin α = A1 kN/m
W2 = P2 kN/m	Seismic active forces
W3 = P3 kN/m	W1 * (k) = A2 kN/m
Total Passive Forces	W2 * (k) = A3 kN/m
P1 + P2 + P3 = **P kN/m**	W3 * (k) = A4 kN/m
Total Interface Length	**Total Active Forces**
L1 + L2 + L3 = **L m**	A1 + A2 + A3 + A4 = **A kN/m**
Friction	Passive Resistance / Active Forces or P/A
Cohesion	Interface Length /Active Forces or L/A

Table 5 : Computations approach for cover slope interface stability

Passive Resistance	Active Forces
S = (W)*cos β = P kN/m	T = (W)*sin β = A1 kN/m
Total Passive Forces	Seismic active
P kN/m	W * (k) = A2 kN/m
Total Interface Length	**Total Active Forces**
L4 = **L m**	A1 + A2 = **A kN/m**
Friction	Passive Resistance / Active Forces or P/A
Cohesion	Interface Length /Active Forces or L/A